Aptamer-based competitive electrochemical biosensor for brevetoxin-2

Shimaa Eissa, Mohamed Siaj, Mohammed Zourob

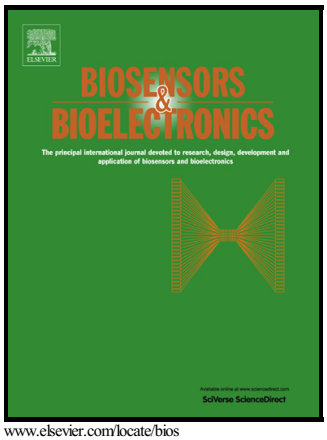

www.elsevier.com/locate/bios

PII: S0956-5663(15)00072-X
DOI: http://dx.doi.org/10.1016/j.bios.2015.01.055
Reference: BIOS7430

To appear in: *Biosensors and Bioelectronic*

Received date: 1 December 2014
Revised date: 22 January 2015
Accepted date: 23 January 2015

Cite this article as: Shimaa Eissa, Mohamed Siaj and Mohammed Zourob, Aptamer-based competitive electrochemical biosensor for brevetoxin-2, *Biosensors and Bioelectronic,* http://dx.doi.org/10.1016/j.bios.2015.01.055

Aptamer-Based Competitive Electrochemical Biosensor for Brevetoxin-2

Shimaa Eissa[a,b], Mohamed Siaj[b], and Mohammed Zourob[c,d*]

[a]Institut National de la Recherche Scientifique, Centre – Énergie, Matériaux et Télécommunications, 1650, Boul. Lionel Boulet, Varennes (Québec) J3X 1S2, Canada, e-mail: shimaaeissa@yahoo.com

[b]Dept. de Chimie et Biochimie, Université du Quebec à Montreal, Montreal, Quebec, Canada H3C 3P8

[c]*Center of Biomedical Engineering*, Cranfield University, Cranfield, Bedfordshire MK43 0AL, UK

[d] Department of Chemistry, Alfaisal University, Riyadh 11533, Kingdom of Saudi Arabia

*Corresponding Author

Email: E: m.zourob@cranfield.ac.uk, Tel.: +44 (0) 1234 758318

Abstract

Brevetoxins (BTXs) are very potent marine neurotoxins that increased in geographical distribution in the past decade causing the illness clinically described as neurological shellfish poisoning (NSP). The ethical problems as well as the technical difficulties associated with the currently employed analysis methods for marine toxins are encouraging the research for suitable

alternatives to be applied in a regulatory monitoring regime. Here, we report an electrochemical biosensor platform for BTX-2 detection utilising aptamer as specific receptor. Using in vitro selection, high affinity DNA aptamers to BTX-2 were successfully selected for the first time from a large pool of random sequences. The binding of BTX-2 to aptamer pools/clones was monitored using fluorescence and electrochemical impedance spectroscopy (EIS). The aptamer BT10 exhibited the highest binding affinity to BTX-2, with a dissociation constant of 42 nM. The effects of the incubation time, pH and metal ions concentrations on the aptamer-toxin binding were studied. The aptamer BT10 was used to construct a label-free competitive impedimetric biosensor for BTX-2 achieving a detection limit of 106 pg/ml. We observed a high degree of cross reactivity of the selected aptamer to the two similar congeners, BTX-2 and -3, whereas no cross reactivity to other marine toxins was obtained. Moreover, the aptasensor was applied for the detection of BTX-2 in spiked shellfish extract showing a very high recovery percentage. We believe that the proposed aptasensor will facilitate the routine detection of BTX-2 in food samples.

Keyword: DNA aptamer, electrochemical Impedance spectroscopy, Aptasensor, In vitro selection

1-Introduction

Brevetoxins (BTXs) are potent cyclic polyether neurotoxins naturally produced by the marine "red tide" dinoflagellates *Karenia brevis* and accumulate in shellfish. BTXs have no toxic effect on shellfish. However, they exhibit toxicity towards marine mammals, birds, fish and humans (Flewelling et al., 2005). BTXs are tasteless, odourless, heat and acid stable. The

exposure of human to BTXs can occur through consumption of contaminated shellfish as well as aerosol exposure in coastal areas. BTX-2 and -3, Fig. S1, are the most predominant forms among ten BTXs that have been isolated and characterized from aerosols, field blooms and *Karenia brevis* cultures (Baden et al., 2005; Landsberg, 2002). BTXs bind to the voltage-gated sodium channels in nerve cells leading to neurologic poisoning and even mortality (Baden et al., 2005). Therefore, the sensitive detection of BTXs in contaminated seafood is of great importance for protecting human health.

Mouse bioassays have been widely considered as a reference method for the detection of most of marine biotoxins including BTXs based on the European regulations (American Public Health Association, 1970; Kreuzer et al., 2002). However, these assays require large number of laboratory animals as well as large amount of tissue extracts to obtain accurate results. Moreover, the poor specificity of these assays is a major drawback that led to growing interest in finding alternative methods. Thus, analytical methods have been developed for the detection of BTXs such as liquid chromatography and mass spectrometry (LC-MS) (Domènech et al., 2014; Hua et al., 1995; Nozawa et al., 2003; Wang and Cole, 2009; Wu et al., 2014). However, these methods are costly, time-consuming and not suitable for on-site monitoring. The successful production of antibodies to BTXs has also allowed the development of several immunological methods. Specifically, Enzyme-linked immunosorbent assay (ELISA) (Naar et al., 2002; Zhou et al., 2010), radioimmunoassay (Poli et al., 1995) and electrochemilumonsence-based immunoassay (Poli et al., 2007) have been developed. Though traditional immunological methods give invaluable insight into BTX presence, they need highly trained personnel and expensive laboratory equipments. Recently, the use of nanomaterials allowed the appearance of few sensitive immunosensors for BTXs detection as promising alternatives to the traditional

immunological methods. For instance, a quartz crystal microbalance immunosensor based on displacement assay using graphene functionalized sensing interface has been reported (Tang et al., 2013). Electrochemical immunosensors for BTXs using gold nanoparticles-decorated dendrimer (Tang et al., 2011) and guanine-functionalized graphene nanoribbons (Tang et al., 2012) have been also developed. However, yet there are major drawbacks associated with the use of antibodies such as their low stability, high cost and complicated in vivo production. These difficulties limit the widespread application of these immunosensing platforms for high-throughput BTXs detection. Hence, developing novel biorecognition receptors for BTXs is of great interest.

Aptamers are single stranded DNA (ssDNA) or RNA oligonucleotides that emerged in the last two decades (Ellington et al., 1990; Tuerk and Gold, 1990) as potential, stable and low cost recognition receptors which can replace antibodies is bioassays. Aptamers are usually selected using systematic evolution of ligands by exponential enrichment (SELEX) technique (Sampson, 2003). The widespread selection of aptamers against many target analytes has lead to the development of various robust biosensing platforms in the recent years (Song et al., 2008). Specifically, due to the increasing awareness of the risk arises from food and water contamination with small molecule toxins, aptamers targeting toxins are being explored (McKeague and DeRosa, 2012). To the best of our knowledge, only two aptamers targeting marine toxins have been selected so far. We have recently reported the selection of an aptamer targeting okadiac acid and its incorporation in a label-free electrochemical biosensing platform (Eissa et al., 2013). Handy et al. (Handy et al., 2013) have also shown the selection of DNA aptamer against saxitoxin. We report herein the first selection, identification and characterization of DNA aptamers against BTX-2. The integration of one of the new selected aptamers in a label-

free competitive electrochemical biosensor was presented. Electrochemical transducers are easy to use, low cost, compatible with modern microfabrication techniques and thus, can be used in developing miniaturized biosensors. We used here Faradaic impedance spectroscopy (EIS), thanks to its high sensitivity and small amplitude perturbation that is safe to the biomolecules. Moreover, EIS is capable of probing the variation in the interfacial properties at the electrode surface upon any modification which offers a label- free mode of detection (Barsoukov and Macdonald, 2005). This novel aptamer-based approach offers a promising, highly stable, low cost and user-friendly strategy that can replace the current sophisticated immunological methods for BTX-2 detection.

2-Experimental

All the materials, reagents and instrumentations used throughout this study are described in details in the supporting information.

2.1. Coupling of brevetoxin-2 to the divinyl sulfone beads

A stock solution of 1mg/ml BTX-2 in DMSO was prepared. 200 µl of the BTX-2 stock solution was diluted to 2 ml with coupling buffer (carbonate buffer, pH 8.5). Two millilitres of DVS beads were washed three times with ultrapure water. The washed beads were then added to the diluted BTX-2 solution in a polypropylene tube and gently mixed end-over-end overnight at room temperature (Fig. S2). After the reaction, the beads were washed three times, two minutes each time with coupling buffer solution to remove the excess unreacted toxin. Then, 4 ml of 0.1 M ethanolamine, pH 9.0 was added to the washed beads and stirred for 2 hours in order to block the unreacted divinyl sulfone groups on the beads. After that the beads were washed extensively with 0.7 M NaCl containing 0.05 % sodium azide to remove the unbound ethanolamine followed

by washing with binding buffer. Simultaneously, negative DVS beads were also blocked using ethanolamine in order to use it for the counter selection rounds. Finally, the positive BTX-2 beads and the negative beads were stored in binding buffer containing 0.02 % sodium azide at 4^{o}C until further use. The success of the immobilization of BTX-2 on the beads was confirmed by performing direct competitive ELISA for the BTX-2-coupled beads and the negative beads as control. ELISA was performed by incubating 10 µl of the washed beads, diluted to 50 µl with PBS buffer (pH 7.4), with sheep anti-BTX antibody that is immobilized on the wells of the microtiter plate. Then, 50 µL of BTX-HRP conjugate solution was added to each well and incubated for 60 minutes. The wells were then washed with the washing buffer provided with the ELISA kit and incubated for 15 minutes with 100 µl of stabilized chromogen (TMB) solution. The detection was based on the competition between the BTX-beads and BTX- HRP conjugate for the binding sites of the antibodies immobilised on the microtiter plate. A blue color was produced in the wells which were incubated with the negative beads whereas, no colour was observed in the wells incubated with the BTX- beads, thereby confirming the success of the coupling reaction. The stability of the BTX-beads were monitored during the SELEX rounds by repeating ELISA experiment several times and all the experiments confirmed the presence of BTX-2 and the stability of the beads over the whole SELEX process.

2.2. Immobilization of Brevetoxin-2 on the gold electrode

Prior to modification, the gold electrodes (2 mm in diameter) were polished with alumina slurry (Al_2O_3) of various particle sizes (1.0, 0.3, and 0.05 µm), followed by washing with Milli-Q water, ultrasonication for 2 min and drying in a nitrogen stream. The electrodes were then cleaned in piranha solution (3:1 mixture of concentrated H_2SO_4 and 30% H_2O_2 for 2 min) and

washed with Milli-Q water. The pretreated gold electrodes were immersed in 10 mM aqueous solution of cysteamine hydrochloride for 12 h at room temperature. After that, the electrodes were washed with absolute ethanol to remove excess cysteamine residues and dried. The terminal amine groups of the cysteamine-modified gold electrodes (Cys/Au) were then activated by immersing the electrodes in 6.5 mM solution of 1,4-phenylene diisocyanate (PDIC) for 2 h at room temperature. Then, the (Cys/ PDIC/Au) electrodes were rinsed with toluene and dried. Five microliters droplet of 100 μg/ml BTX-2 solution in DMSO was immediately added onto the (Cys/ PDIC/Au) electrodes surface and incubated for 2 hours (Scheme 1A). The electrodes were extensively washed with methanol to remove the unreacted BTX-2. The remaining free isocyanate groups were then blocked by immersing the electrodes into methanol for 5 hours. The BTX-modified electrodes (BTX electrodes) were washed with water and stored at 4 ^{o}C in binding buffer until further use.

Scheme 1

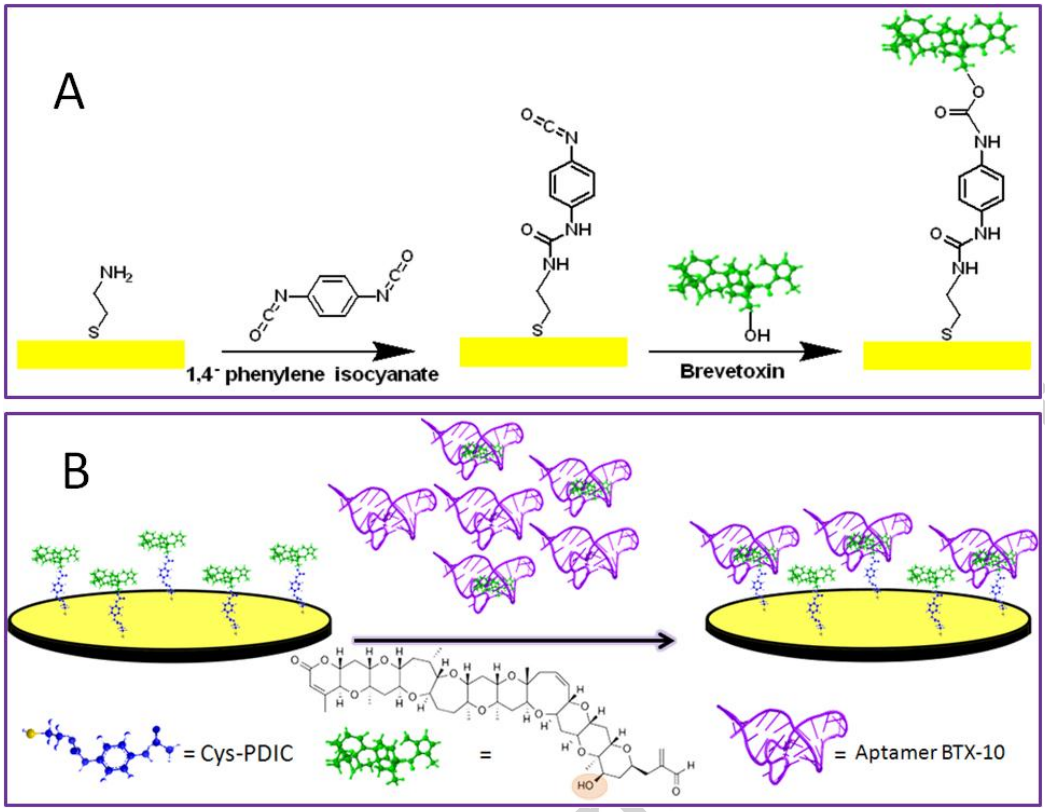

2.3. In vitro selection of the DNA Aptamer

The selection of the aptamers was performed according to the protocol described in Fig. S3. Then, cloning, sequencing and binding analysis of the selected DNA were performed as explained in details in the supporting information.

2.4. Electrochemical competitive assay

For the BTX-2 detection assay, specificity, cross reactivity and real sample experiments, the BTX electrodes were incubated for 30 min with 5 µL of 500 nM BT10 aptamer mixed with specific concentrations of BTX-2, BTX-3, okadaic acid (OA), microcystin-LR (MC-LR)

standard solutions or mussel extracts prepared as explained in the supporting information and spiked with BTX-2 (Scheme 1B). The electrodes were then washed with binding buffer and subjected to electrochemical measurements. The cyclic voltammetry (CV) experiments were conducted at a scan rate of 100 mV/s. The electrochemical impedance spectroscopy (EIS) were recorded over a frequency range from 10 kHz to 1.0 Hz using an alternative voltage with amplitude of 10 mV, superimposed on a DC potential of 0.20 V (*vs* a Ag/AgCl reference electrode).The impedance data were plotted in the form of complex plane diagram (Nyquist plot). The obtained spectra were fitted using the Nova 1.9 software. All the EIS and CV measurements were recorded in a 0.1 M PBS buffer solution containing 5 mM $[Fe(CN)_6]^{3-/4-}$ redox pair (1:1 molar ratio).

3. Results and discussion

3.1. Immobilization of brevetoxin-2 on the divinyl sulfone activated beads

The attachment of target to solid matrix is usually necessary to enable the separation of bound from unbound DNA through the selection process particularly for small molecule targets. The immobilization of BTX-2 on divinyl sulfone beads was achieved by coupling the terminal DVS groups on the beads with the hydroxyl groups on the BTX-2 molecules (Fig. S2). The choice of the hydroxyl group as anchoring point of the BTX-2 molecule is used to retain the rest of the molecule accessible for DNA binding during the SELEX. This hydroxyl function is common in all BTX congeners, which may enable similar aptamer selection against the other congeners in the future. The success of the coupling reaction was then confirmed using direct competitive ELISA.

3.2. Immobilization of Brevetoxin-2 on the gold electrodes

BTX-2 was also immobilized on the gold electrode surface via its hydroxyl group in order to keep the same exposition site of the molecules for the DNA binding as that used on the beads. First, The gold surface was functionalized through the formation of self-assembled monolayer (SAM) of Cysteamine. Then, the bifunctional linker, 1,4-phenylene diisocyanate (PDIC), was used to covalently attach the terminal amine groups of Cys/Au to the hydroxyl groups of the BTX-2 molecules (Scheme 1A). This linker offers high stability, low toxicity and capability to react efficiently with the amine groups yielding carbamide moiety as well as the hydroxyl groups yielding carbamate (urethane) moiety (Aissaoui et al., 2013; Persson et al., 2001). To confirm the successful modification of the gold electrodes and the subsequent immobilization of the BTX-2 molecules, CV and EIS were used. Fig. 1A shows cyclic voltammograms in $[Fe(CN)_6]^{3-/4-}$ redox couple at bare Au electrode, Cys/Au and after activation with PDIC and immobilization of BTX-2. As expected, the CV of $[Fe(CN)_6]^{3-/4-}$ redox solution showed a reversible behaviour on the bare Au electrode with a peak-to peak separation (ΔE) of 80 mV. After the self assembly of cysteamine, the peak current was slightly increased and the ΔE was decreased likely due to the electrostatic attraction between the $[Fe(CN)_6]^{3-/4-}$ anions and the positively charged terminal amine groups of the Cys/Au (Tlili et al. 2013). However, after the activation of the amine groups with the PDIC linker and immobilization of BTX-2, a drop in the peak current and an increase in the ΔE were observed, presumably due to the blocking of the surface with the BTX molecules leading to retardation of the electron transfer. Likewise, EIS was used to characterize the stepwise modification of the Au electrodes. Fig. 1B shows the Faradiac impedance spectra in $[Fe(CN)_6]^{3-/4-}$ solution represented as Nyquist plots. The plots are characterized by a semicircle at high frequencies, corresponding to the electron transfer-limited

process and a straight line at lower frequencies, representing the diffusion process. A modified Randles equivalent circuit (shown in the inset of Fig. 1B) was used for fitting the impedance spectra (explained in the Supporting Information). The R_{CT} is usually the most sensitive electrical element that can be used to characterize the events occurring at the electrode interface (Danielsa and Pourmanda, 2007). The self assembly of cysteamine on the electrode resulted in a decrease in the R_{CT} to a value of 45± 6.2 Ω than the bare gold electrode (117±5.7 Ω) and only a straight line was observed confirming the enhancement of the electron transfer due to the introduction of the positive amine groups to the surface. On the other hand, the immobilization of BTX led to remarkable increase in R_{CT} to 398±4 Ω as a result of the blocking effect of the toxin molecules that causes hindrance to the flow of the redox probe to the gold surface. Hence, the results obtained from both EIS and CV confirms the successful immobilization of BTX molecules on the gold electrode.

Fig. 1.

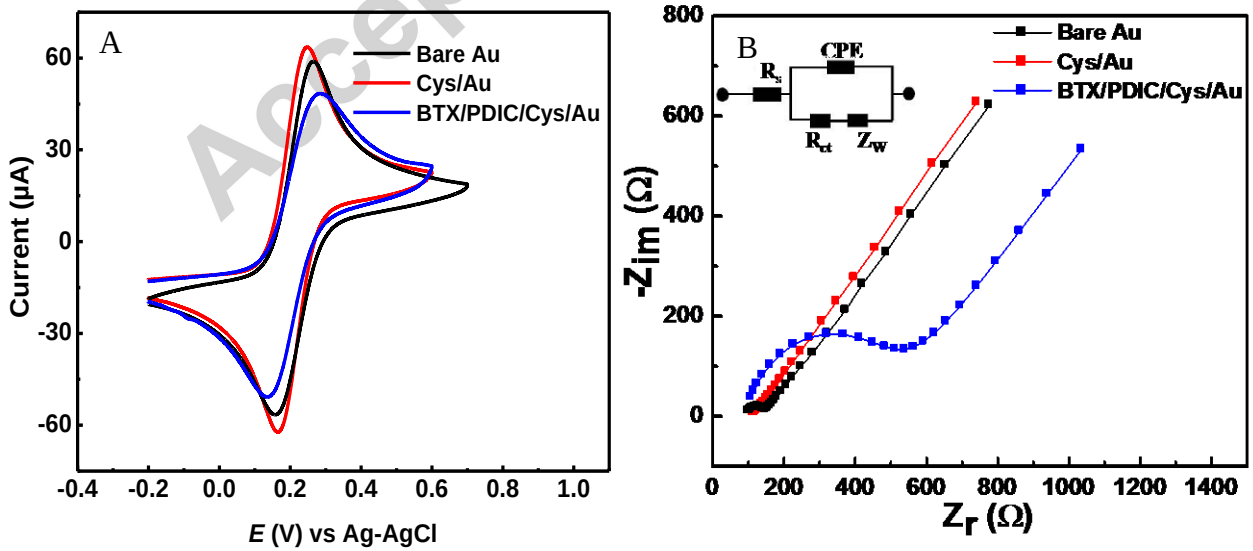

3.3. In Vitro Selection of the DNA aptamers

The aptamers selection was performed using a DNA library consists of 1.8×10^{15} random 60-nucleotide sequences. As explained in details in the Supporting Information, five consecutive steps were carried out in each round: (1) incubation of the random library with the BTX-beads, (2) separation of the unbound an weakly bound DNA to the BTX- beads by washing, (3) Elution of the bound DNA sequences to BTX, (4) Desalting and PCR amplification of the eluted DNA pool and (5) purification of the fluorescent ssDNA (aptamer) from the PCR product using denaturing PAGE. Two successive counter selection steps after the seventh and eighth rounds were introduced against negative DVS beads, which were used as a matrix for immobilizing the BTX-2. The purpose of these counter selection rounds was to eliminate the ssDNA sequences that were nonspecifically bound to the beads matrix.

In order to monitor the enrichment of the specific DNA to BTX-2 during the SELEX rounds, both fluorescence and EIS methods were utilized. The amount of bound DNA was assessed by measuring the fluorescence of the eluted DNA in each round. Moreover, the binding was evaluated by measuring the % R_{CT} change after incubating the PCR amplified pools with BTX electrodes. The binding of the DNA to BTX electrodes leads to an increase in the total negative charge due to the phosphate backbone of the DNA which retards the access of the $[Fe(CN)_6]^{3-/4-}$ anions to the electrode surface and thus increases the R_{CT}. As shown in Fig. 2A, a progressive increase in the DNA binding was noticed throughout the selection rounds as demonstrated by the fluorescence and the EIS measurements, suggesting the gradual enrichment of the DNA pools with the specific sequences. We have not seen any diminution in the DNA binding after the counter selection steps which indicates that no signification enrichment in the

nonspecifically bound DNA to the DVS beads has occurred. However, a remarkable increase in the bound DNA was observed in the last three rounds where the binding reached a plateau, suggesting enrichment in the specific aptamers for BTX-2. Therefore, the DNA pool from round 10 was cloned and 27 clones were randomly chosen for sequencing. The identified sequences were analysed by multiple sequence alignment using PRALINE software (Simossis et al., 2005). A significant sequence convergence in the DNA pool from round 10 sequences was observed confirming the successful enrichment of that pool. Six different families (A-F) were identified according to their similarities showing high degree of homology among the members of each group (Fig. S4).

Fig. 2.

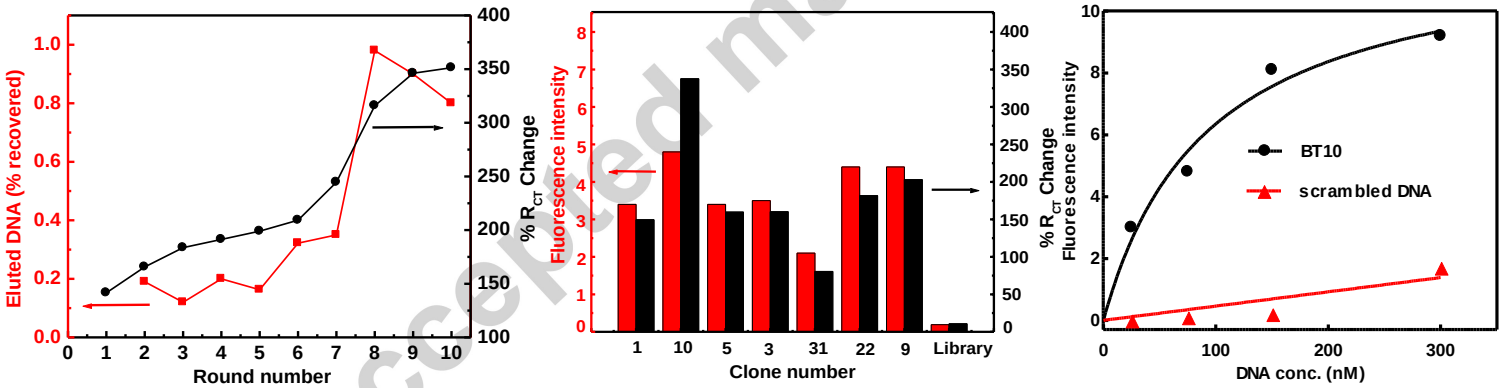

3.4. Binding affinity analysis of the aptamers

Representative sequences from each group were chosen for further binding analysis. Initial screening of the selected aptamer clones (BT 1, 10, 5, 3, 31, 22, 9) to confirm their successful binding to BTX-2 using fluorescence as well as EIS was performed. Fig. 2B shows a comparative estimation of the relative binding ability of each aptamer clone to BTX-2 based on the fluorescence measurement of the eluted DNA from the beads as well as the % change of the

R_{CT} of BTX electrodes upon binding. Specific binding of all the tested aptamer clones to the BTX-2 was observed compared to binding of the initial library (Control pool). We then determined the binding affinity of the selected aptamers using a fluorescence binding assay. A constant amount of BTX-2 beads and different concentrations of fluorescein-labelled aptamers (0-300 nM) were used to evaluate the dissociation constant of the aptamers under the same conditions which were used for selection. As shown in Fig. 2C, by plotting the fluorescence intensity of the eluted DNA versus the aptamer concentration, the K_d was calculated using non linear regression analysis. A scrambled DNA sequence was used as a control for the binding experiments showing non-significant binding to the BTX-beads. Table 1 shows the calculated K_d values of the selected aptamers ranging from 92 to 1296 nM. It was observed that the aptamer BT10 have shown the highest binding affinity to BTX-2 (K_d= 92 nM), therefore, it was chosen for our application. The secondary structure predictions for the BT10 aptamer sequence without the primer binding regions is shown in Figure S5.

3.5. Optimization of the aptamer-toxin binding conditions

With the aim to shed a light on the factors which can influence the BT10 aptamer-toxin binding and to optimise the binding conditions for achieving the highest possible affinity, the incubation time, sodium and magnesium ions concentrations, and the pH of the binding buffer were studied. Fig. 3A shows the % R_{CT} change of the BTX electrodes after incubation with 500 nM BTX-2 at different time points. An enhancement in the % R_{CT} change was observed until 30 min binding time when saturation was reached.

Fig. 3.

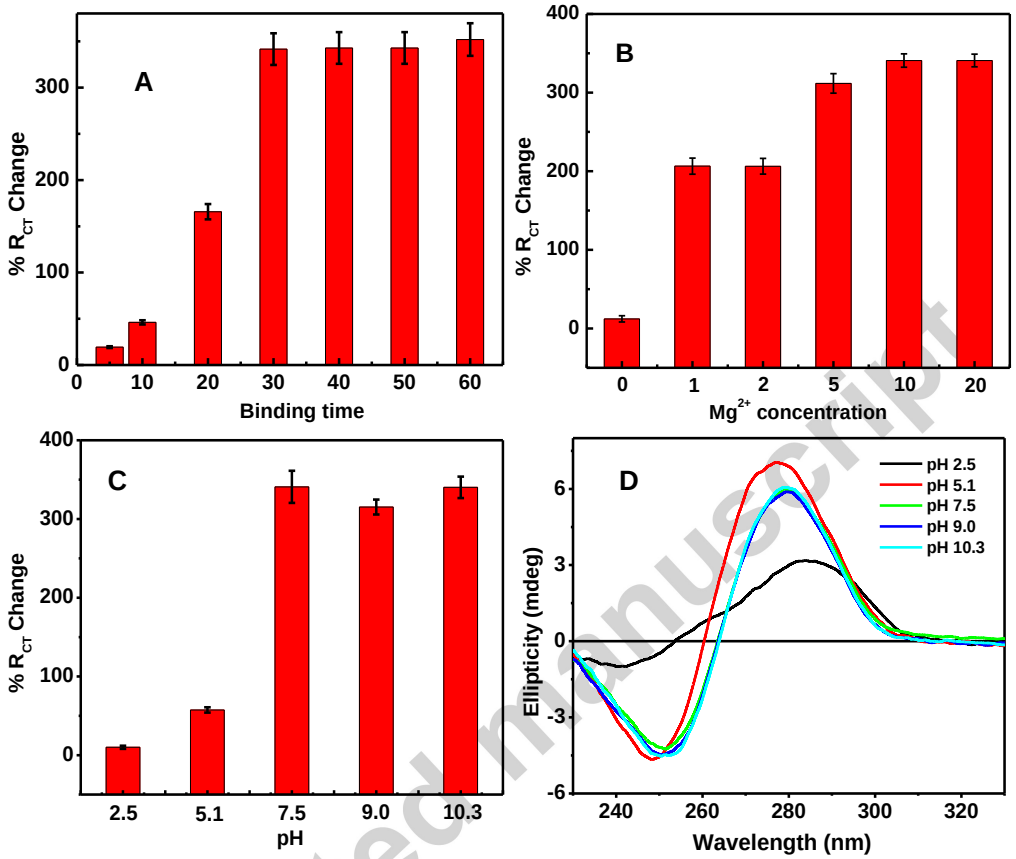

Fig. 3B shows a clear dependence of the aptamer-toxin binding on the Mg^{2+} concentration which is in agreement with previous studies on other aptamers (Cruz-Aguado and Penner, 2008; Eissa et al., 2014). An increase in the R_{CT} with increasing the concentration of Mg^{2+} cations was observed until 10 mM Mg^{2+} after which no further change was seen. Such affinity change is likely due to the effect of Mg^{2+} on the DNA conformation. On the other hand, by changing the concentration of sodium ions in the binding buffer from 0-200 mM, no effect on the aptamer-toxin binding have been observed (data not shown). Fig. 3C shows the effect of pH of the binding buffer on the aptamer-toxin binding monitored by the % change in the R_{CT} (Fig. 3D). It

was clearly observed that the binding of the aptamer to BTX-2 was significantly diminished at acidic pHs (2.5, 5.1). However, no significant effect on the binding at pH > 7.5 was seen. To better understand the origin of such effect, systematic circular dichroism spectra of the aptamer at different pHs were recorded (Fig. 3D). A comparable spectra of the aptamer at pHs > 7.5, in comparison to significant difference in the spectra in acidic pHs confirms the important role of the pH on the DNA aptamer conformation, and consequently, the binding with BTX-2. Therefore, an incubation time of 30 min and binding buffer which consists of 50 mM Tris, pH 7.5, and 10 mM $MgCl_2$ were used in the subsequent experiments to improve the affinity and to enhance the signal associated with the aptamer-toxin binding. Under these optimum conditions, we have again estimated the binding affinity of the BT10 aptamer and a K_d value of 42 nM was obtained.

3.6. Electrochemical Competitive Aptasensor

The aptamer with the highest affinity, BT10, was assessed for the detection of BTX-2 in a label-free electrochemical competitive assay. The competition was established between the immobilized BTX-2 on the gold electrode and free BTX-2 in solution in the presence of a fixed amount of the aptamer. The electrochemical detection was realized based on the change of R_{CT} of the $[Fe(CN)_6]^{4-/3-}$ redox couple. With increasing the concentration of BTX-2 in solution, the amount of free aptamer available for binding to the immobilized BTX-2 on the gold surface decreases resulting in lower R_{CT} change. Since the aptamer concentration used for the competition step is a crucial factor in the aptasensor fabrication, it was important to perform initial optimization of the aptamer concentration without competition. Generally, higher aptamer

concentration will lead to decreased sensitivity and lower aptamer concentration will lead to reduced signal value (Hayat et al., 2011). Based on our optimization experiment, a concentration of 500 nM BT10 aptamer was chosen to strike a balance between the two effects. Fig. 4A shows the decrease in the R_{CT} with increasing the concentration of BTX-2 from 0.01 to 2000 ng/ml.

Fig. 4.

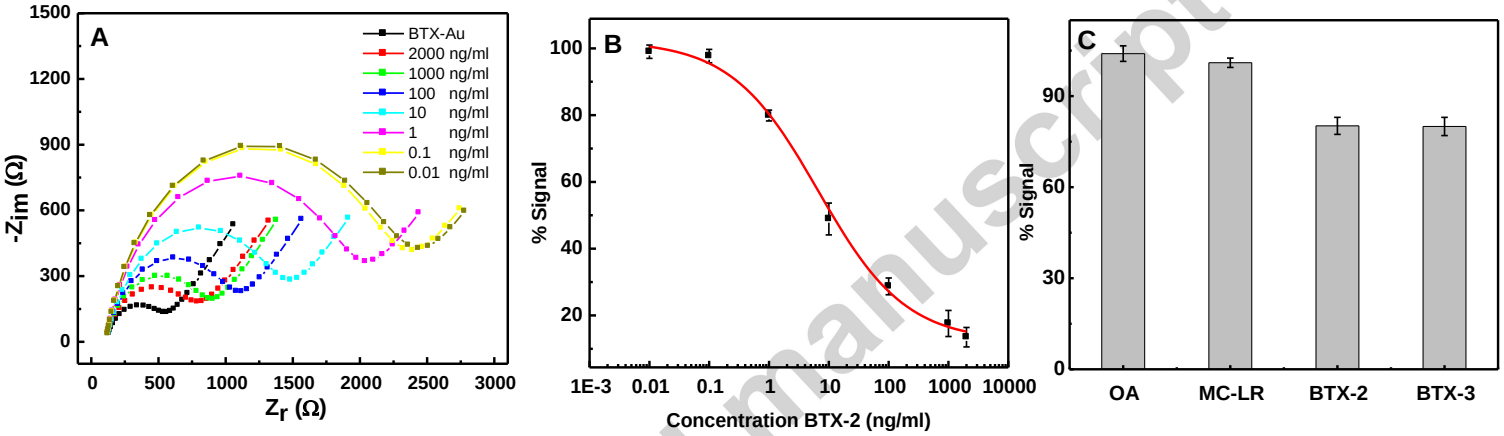

A sigmoidal dose response curve was obtained (Fig. 4B) by plotting the analytical response (% signal) expressed as a percentage of the maximum signal obtained when no BTX-2 was added $[(R_{CT}-R_I)/(R_{max}-R_I)\times100]$ *vs.* toxin concentration. R_{CT} is the resistance after incubation with certain concentration of BTX-2, R_{max} is the resistance at zero BTX-2 and R_I is the background signal of the BTX electrode. The calibration curve was fitted to a sigmoidal logistic four-parameter equation:

$$Y = \mathrm{A} + \frac{(\mathrm{B} - \mathrm{A})}{1 + \left(\frac{\mathrm{x}}{\mathrm{EC50}}\right)^{\mathrm{b}}}$$

where A, B are the minimum and maximum analytical response, respectively. b is the slope at the inflection point and EC50 is the concentration leading to 50% of the maximum signal. The

best-fit values of the experimental data are the following: y = 12.2 +(102.35− 12.2)/(1 + (x/6.66)0.59), with a correlation coefficient R^2= 0.997. The limit of detection (LOD) was calculated as the concentration that leads to 95% of the maximum signal to be 106 pg/ml. This LOD is comparable with the LOD of reported aptasensors for other small molecules (Eissa et al., 2013) as well as the previously reported electrochemical immunosensor for BTX-2 (Tang et al., 2011). However, compared to the present work, the reported work uses much more complicated sensor designs and signal amplification reagents.

Cross reactivity experiment with BTX-3, a similar analogue to BTX-2 (Fig. S1), and negative control experiments with OA and MC-LR were studied using 1 ng/ml of each toxin. As shown in Fig. 4C, the aptasensor analytical response was comparable for both BTX-2 and BTX-3 indicating high degree of cross reactivity which can be exploited to detect the total concentrations of both congeners in a sample similar to the case of immunoassays. However, a high response, close to the maximum signal was obtained with MC-LR and OA due to the non significant interference of these toxins with the competitive assay, which indicates the high selectivity of the aptasensor.

3.7. Analysis of brevetoxin-2 in Real Shellfish Samples

In order to demonstrate the feasibility of detecting BTX-2 in food matrix, a spiked shellfish extracts were analyzed using the developed aptasensor. As shown in Table S1 in the Supporting Information, a good recovery percentage was obtained for BTX-2 in the shellfish extracts indicating non significant interference from the shellfish matrix on the aptasensor response. Thus, these results confirm the possible applicability of the developed apasensor in real sample analysis.

4. **Conclusions**

High affinity DNA aptamers for BTX-2 were successfully selected for the first time using SELEX from large pool of random library. After ten rounds of selection the initial pool was enriched in the high affinity sequences as monitored using fluorescence as well as impedance measurements. All the tested aptamers could bind BTX-2 with dissociation constants in the nanomolar range under the SELEX conditions. The highest affinity aptamer BT10, K_d = 42 nM under the optimum binding condition, was applied for the detection of BTX-2 in an electrochemical competitive aptasensor showing remarkable sensitivity. Moreover, the aptasensor showed good selectivity to BTX-2 against other toxins from different groups such as okadiac acid and microcystins. However, high degree of cross reactivity between the two similar analogues BTX-2 and BTX-3 was observed. We believe that the simplicity along with the improved stability and lower cost of the proposed aptasensor will help to facilitates the routine quantification of the two most predominant forms of BTXs, BTX-2 and BTX-3, in shellfish. Several different truncation series of the aptamer will be studied in the future to ascertain which part among the full aptamer sequence was essential for the target binding which can be useful for further applications.

References

APHA, 1970. Recommended Procedures for the Examination of Sea Water and Shellfish, 4th Ed., in: Greenberg, A.E., Hunt, D.A. (Eds), American Public Health Association, Washington, DC, pp. 61–66.

Barsoukov, E., Macdonald, J. R., 2005. Impedance Spectroscopy: Theory, Experiment, and Applications, John Wiley & Sons, New York.

Ellington, A. D., Szostak, J. W., 1990. Nature 346, 818-822.

Naar, J., Bourdelais, A., Tomas, C., Kubanek, J., Whitney, P. L., Flewelling, L., Steidinger, K., Lancaster, J., Baden, D. G., 2002. Environ. Health Perspect. 110, 179-185.

Poli, M. A., Rein, K. S. Baden, D. G., 1995. J. AOAC Int. 78, 538-542.

Poli, M. A., Rivera, V. R., Neal, D. D., Baden, D. G., Messer, S. A., Plakas, S. M., Dickey, R. W., Said, K. E., Flewelling, L., Green, D., White, J., 2007. J. AOAC Int. 90, 173-178.

Simossis, V. A., Kleinjung, J., Heringa, 2005. Nucleic Acids Res. 33, 816-824.

Tuerk, C., Gold, L., 1990. Science 249, 505-510.

Zhou, Y., Li, Y-S., Pan, F-G., Zhang, Y-Y., Lu, S-Y., Ren, H-L., Li, Z-H., Liu, Z-S., Zhang, J-H., 2010. Food Chem. 118, 467-471.

Aissaoui, N., Landoulsi, J., Bergaoui, L., Boujday, S., Lambert, J.-F., 2013. Enzyme Microb. Tech. 52, 336-343.

Baden, D.G., Bourdelais, A.J., Jacocks, H., Michelliza, S., Naar, J., 2005. Environ. Health Perspect. 113, 621–625.

Cruz-Aguado, J.A., Penner, G., 2008. J. Agric. Food Chem. 56, 10456-10461.

Danielsa, J.S., Pourmanda, N., 2007. Electroanalysis 19, 1239–1257.

Domènech, A., Cortés-Francisco, N., Palacios, O., Franco, J.M., Riobó, P., Llerena, J.J., Vichi, S., Caixach, J., 2014. J. Chromatogr. A 1328, 16-25.

Eissa, S., Ng, A., Siaj, M., Tavares, A.C., Zourob, M., 2013. Anal. Chem. 85, 11794-11801.

Eissa, S., Ng, A., Siaj, M., Zourob, M., 2014. Anal. Chem. 86, 7551-7557.

Flewelling, L.J., Naar, J.P., Abbott, J.P., Baden, D.G., Barros, N.B., Bossart, G.D., Bottein, M.-Y.D., Hammond, D.G., Haubold, E.M., Heil, C.A., Henry, M.S., Jacocks, H.M., Leighfield, T.A., Pierce, R.H., Pitchford, T.D., Rommel, S.A., Scott, P.S., Steidinger, K.A., Truby, E.W., Van Dolah, F.M., Landsberg, J.H., 2005. Nature 435, 755-756.

Handy, S.M., Yakes, B.J., DeGrasse, J.A., Campbell, K., Elliott, C.T., Kanyuck, K.M., DeGrasse, S.L., 2013. Toxicon 61, 30-37.

Hayat, A., Barthelmebs, L., Sassolas, A., Marty, J.-L., 2011. Talanta 85, 513-518.

Hua, Y., Lu, W., Henry, M.S., Pierce, R.H., Cole, R.B., 1995. Anal. Chem. 67, 1815-1823.

Kreuzer, M.P., Pravda, M., O'Sullivan, C.K., Guilbault, G.G., 2002. Toxicon 40, 1267-1274.

Landsberg, J.H., 2002. Rev. Fish. Sci. 10, 113-390.

McKeague, M., DeRosa, M.C., 2012. J. Nucleic Acids 2012, 748913.

Nozawa, A., Tsuji, K., Ishida, H., 2003. Toxicon 42, 91-103.

Persson, H.H.J., Caseri, W.R., Suter, U.W., 2001. Langmuir 17, 3643-3650.

Sampson, T., 2003. World Pat. Inf. 25, 123-129.

Song, S., Wang, L., Li, J., Fan, C., Zhao, J., 2008. TrAC Trend. Anal. Chem. 27, 108-117.

Tang, D., Tang, J., Su, B., Chen, G., 2011. Biosens. Bioelectron. 26, 2090-2096.

Tang, D., Zhang, B., Tang, J., Hou, L., Chen, G., 2013. Anal. Chem. 85, 6958-6966.

Tang, J., Hou, L., Tang, D., Zhou, J., Wang, Z., Li, J., Chen, G., 2012. Biosens. Bioelectron. 38, 86-93.

Tlili, C., Sokullu, E., Safavieh, M., Tolba, M., Ahmed, M.U., Zourob, M., 2013. Anal. Chem. 85, 4893-4901.

Wang, W., Cole, R.B., 2009. Anal. Chem. 81, 8826-8838.

Wu, H., Guo, M., Tan, Z., Cheng, H., Li, Z., Zhai, Y., 2014. J. Chromatogr. A 1358, 172-180.

Figure Captions

Fig. 1. Cyclic voltammetry **(A)** and Nyquist plots **(B)** of 5 mM $[Fe(CN)_6]^{4-/3-}$ redox couple in PBS, pH 7.4, for bare Au electrode (black), Cys/Au (red) and BTX/PDIC/Cys/Au (blue). The cyclic voltammetry was performed at scan rate of 100 mV/s and the EIS was performed using a frequency range of 10^4 to 0.1 Hz, a DC potential of +0.20 V and AC amplitude of 10 mV. The inset in **Figure1B** is the equivalent circuit applied to fit the impedance spectra.

Fig. 2. (A) Binding of ssDNA pools to BTX-2 after each selection round monitored by calculating the recovery percentage from the fluorescence of eluted DNA (red) and % R_{CT} change ; $(R_{CT}-R_I)/R_I$%; of the BTX electrodes after binding (black). (B) Binding assays with the individual aptamer clones BTX 1, 10, 5, 3, 31, 22 and 9, to test their ability to bind to BTX-beads (red) and BTX electrodes (black). The unenriched initial library was used as the negative control. (C) Fluorescence binding curve of BTX-2 to aptamer BT10 (black) and a scrambled DNA sequence (red).

Fig. 3. The effect of incubation time (A), Mg^{2+} ions concentration (B) and pH of the binding buffer (C) on BTX-aptamer binding, monitored by measuring the % R_{CT} change in10 mM PBS

(pH 7.4) containing 5 mM $[Fe(CN)_6]^{4-/3-}$ redox couple after incubating the BTX electrodes with 500 nM aptamer. The error bars represent the standard deviation of the measurements. (D) The CD spectra of the BTX aptamer in binding buffer with different pHs.

Fig. 4. (A) Nyquist plots of the BTX electrode before and after incubation with different concentrations of BTX-2 mixed with 500 nM aptamer (B). The calibration curve for BTX-2, plot of analytical response (% Signal, $[(R_{CT} - R_I)/(R_{max} - R_I) \times 100]$) *vs.* BTX-2 concentration. The error bars show the standard deviation of two repetitive measurements. **(C)** Comparison of response of the aptasensor to 1 ng/ml BTX-2, BTX-3, MC-LR, and OA.

Scheme 1 (A) Modification of the gold electrode surface and covalent immobilization of BTX-2, (B) the working principal of the aptasensor with competitive assay.

Table 1. Sequences and dissociation constants (K_d) between BTX-2 and selected aptamers.

Group	Clone number	**Aptamer sequence**	**K_d (nM)**
A	BT 1	CACACCAAACACACAAGTGGACCCTGACGCATGGATAGGGTGACGGTATACGCGGGCATG	385
	BT 10	GGCCACCAAACCACACCGTCGCAACCGCGAGAACCGAAGTAGTGATCATGTCCCTGCGTG	92
B	BT 5	CACGGGCAGAGGGATAGGTTGTTGACGGGGCTGGTGGGTGGGTGCGCTCGCGCTATCGTGG	311
C	BT 3	GGCGATAGGCAGTGTTGCGGGGTCGGAGAGCGAGGTAATAGCGTGTATGGGTGCTGTGTG	278
D	BT 31	ACCACCGGCCCGAGATAGTCTAGACCACTATGTTGTTGTGCTTACTGCTGTGTGGTGTGG	1296
E	BT 22	GGCCACACAAACAACATGACAACACGTCTCACATAACGCCCACGTGCTGCCGCCTCATCG	258
F	BT 9	TCACGAGAGAGCGAGAGCGCCCCCCCACCACAGCCGTCACCACCCTATTCCTCTGCCGTTG	166

Highlights

- High affinity DNA aptamers for Brevetoxin-2 were successfully selected for the first time using SELEX from large pool of random library.
- All the tested aptamers could bind to BTX-2 with dissociation constants in the nanomolar range.
- The highest affinity aptamer was applied for the detection of BTX-2 in an electrochemical competitive aptasensor showing remarkable sensitivity.
- The aptasensor was applied for the detection of BTX-2 in spiked shellfish extract showing a very high recovery percentage.